

## Electronic Supplementary Information

# **Pb<sub>2</sub>B<sub>10</sub>O<sub>16</sub>(OH)<sub>2</sub>·B(OH)<sub>3</sub>·H<sub>2</sub>O: Enhanced Second Harmonic Generation Significantly via Substituting Metal Cations in Isostructural Compounds with Pb<sup>2+</sup>**

Xintong Cai,<sup>a, b</sup> Kaitong Liu<sup>a, b, \*</sup> and Yanhui Zhang,<sup>a, b \*</sup>

<sup>a</sup>Xinjiang Key Laboratory for Luminescence Minerals and Optical Functional Materials, School of Physics and Electronic Engineering, Xinjiang Normal University, Urumqi, Xinjiang 830054, China.

<sup>b</sup>College of Chemistry and Chemical Engineering, Xinjiang Normal University, Urumqi, Xinjiang 830054, China.

\* Corresponding author: liukaitong@xjnu.edu.cn, zyh0403@xjnu.edu.cn.

## CONTENTS

### Experimental section

**Table S1.** Crystal data and structure refinement for  $\text{Pb}_2\text{B}_{10}\text{O}_{16}(\text{OH})_2\cdot\text{B}(\text{OH})_3\cdot\text{H}_2\text{O}$

**Table S2.** Atomic coordinates and displacement parameters for  $\text{Pb}_2\text{B}_{10}\text{O}_{16}(\text{OH})_2\cdot\text{B}(\text{OH})_3\cdot\text{H}_2\text{O}$

**Table S3.** Hydrogen coordinates ( $\times 10^4$ ) and isotropic displacement parameters ( $\text{Å}^2 \times 10^3$ ) for  $\text{Pb}_2\text{B}_{10}\text{O}_{16}(\text{OH})_2\cdot\text{B}(\text{OH})_3\cdot\text{H}_2\text{O}$

**Table S4.** Hydrogen bonds for  $\text{Pb}_2\text{B}_{10}\text{O}_{16}(\text{OH})_2\cdot\text{B}(\text{OH})_3\cdot\text{H}_2\text{O}$

**Table S5.** Bond lengths and angles for  $\text{Pb}_2\text{B}_{10}\text{O}_{16}(\text{OH})_2\cdot\text{B}(\text{OH})_3\cdot\text{H}_2\text{O}$

**Table S6** Assignments of the infrared absorption bands for  $\text{Pb}_2\text{B}_{10}\text{O}_{16}(\text{OH})_2\cdot\text{B}(\text{OH})_3\cdot\text{H}_2\text{O}$

**Table S7.** A comprehensive study on the structural and performance characteristics of reported hydrated borates containing Pb element

**Table S8.** Dipole moment calculations of BO groups

**Table S9.** Atom-cutting analysis of nonlinear coefficients  $d_{22}$

**Figure S1.** Powder XRD of  $\text{Pb}_2\text{B}_{10}\text{O}_{16}(\text{OH})_2\cdot\text{B}(\text{OH})_3\cdot\text{H}_2\text{O}$

**Figure S2.** The arrangements and link mode of Pb1 and Pb2 in  $\text{Pb}_2\text{B}_{10}\text{O}_{16}(\text{OH})_2\cdot\text{B}(\text{OH})_3\cdot\text{H}_2\text{O}$

**Figure S3.** The distances between  ${}^2[\text{B}_5\text{O}_{10}(\text{OH})]_{\infty}$  layers in  $\text{M}_2\text{B}_{10}\text{O}_{16}(\text{OH})_2\cdot\text{B}(\text{OH})_3\cdot\text{H}_2\text{O}$  (M = Pb, Ba, Sr, and Ca)

**Figure S4.** The shortest phase-matching length and calculated birefringence of  $\text{Pb}_2\text{B}_{10}\text{O}_{16}(\text{OH})_2\cdot\text{B}(\text{OH})_3\cdot\text{H}_2\text{O}$

**Figure S5.** The arrangements of  $[\text{BO}_3]$  triangles and the  $n_x$ ,  $n_y$ ,  $n_z$  direction in  $\text{Pb}_2\text{B}_{10}\text{O}_{16}(\text{OH})_2\cdot\text{B}(\text{OH})_3\cdot\text{H}_2\text{O}$  unit cell

## **Experimental section**

### **1. Crystal growth**

$\text{Pb}_2\text{B}_{10}\text{O}_{16}(\text{OH})_2\cdot\text{B}(\text{OH})_3\cdot\text{H}_2\text{O}$  was synthesized via conventional hydrothermal method.  $\text{PbO}$  and  $\text{H}_3\text{BO}_3$  were weighed as raw materials according to the molar ratio of 2: 11. Whereafter the raw material was mixed thoroughly, then transferred and sealed into a pouch made of tetrafluoroethylene. The pouch was put in a 100 ml Teflon hydrothermal reactor and heated to 220 °C slowly in an oven, then held for 3 days. Subsequently, the oven was cooled to 110 °C at the rate of 2.7 °C/h and then decreased to room temperature at the rate of 10 °C/h. The colourless crystals are obtained after cleaning with deionized water, with a yield of 92% based on Pb.

### **2. Single-crystal X-ray diffraction**

A suitable size high-quality colorless crystal was selected via a polarizing microscope and then mounted on a thin glass fiber, which was investigated by Bruker D8 Venture diffractometer using monochromatic Mo  $K\alpha$  radiation ( $\lambda = 0.71073 \text{ \AA}$ ) at 293(2) K. Single-crystal XRD data were integrated with the SAINT-Plus program. All calculations were performed with programs from the SHELXTL crystallographic software package.<sup>1</sup> The structure of  $\text{Pb}_2\text{B}_{10}\text{O}_{16}(\text{OH})_2\cdot\text{B}(\text{OH})_3\cdot\text{H}_2\text{O}$  was refined with direct methods and verified by PLATON software to check whether having higher symmetrical elements.<sup>2</sup>

### **3. Powder X-ray diffraction**

Powder X-ray diffraction (XRD) of  $\text{Pb}_2\text{B}_{10}\text{O}_{16}(\text{OH})_2\cdot\text{B}(\text{OH})_3\cdot\text{H}_2\text{O}$  polycrystalline was implemented on a Bruker D2 PHASER diffractometer equipped with a Cu  $K\alpha$  ( $\lambda = 1.54056 \text{ \AA}$ ) radiation diffracted beamed monochromator with a scan step width of 0.02° in the 2 $\theta$  range from 5 to 70° at room temperature and a fixed counting time of 1 s/step.

### **4. Infrared spectrum**

A Shimadzu IR Affinity-1 FTIR spectrometer was used to record the infrared (IR) spectrum of  $\text{Pb}_2\text{B}_{10}\text{O}_{16}(\text{OH})_2\cdot\text{B}(\text{OH})_3\cdot\text{H}_2\text{O}$  at room temperature in the range 400-4000  $\text{cm}^{-1}$  to identify the functional groups, and the sample with dried KBr was mixed thoroughly at a mass ratio of 1: 100.

### **5. UV-Vis-NIR diffuse-reflectance spectrum**

A SolidSpec-3700DUV spectrophotometer was applied to collect the UV-Vis-NIR diffuse-reflectance spectrum for  $\text{Pb}_2\text{B}_{10}\text{O}_{16}(\text{OH})_2\cdot\text{B}(\text{OH})_3\cdot\text{H}_2\text{O}$ . A polycrystalline sample smooth wafer with a thickness of 0.5 millimeters was used to measure the spectrum at room temperature in the wavelength range of 190 to 1900 nanometers.

### **6. Thermal analysis**

Thermal gravimetric (TG) and differential scanning calorimetry (DSC) of  $\text{Pb}_2\text{B}_{10}\text{O}_{16}(\text{OH})_2 \cdot \text{B}(\text{OH})_3 \cdot \text{H}_2\text{O}$  polycrystalline samples were carried out on a NETZSCH STA 449C thermal analyzer instrument. The sample was placed in a platinum crucible and heated from 40 to 600 °C at a rate of 10 °C/min in an atmosphere with flowing nitrogen.

## 7. Powder SHG measurement

The SHG response of  $\text{Pb}_2\text{B}_{10}\text{O}_{16}(\text{OH})_2 \cdot \text{B}(\text{OH})_3 \cdot \text{H}_2\text{O}$  polycrystalline samples was characterized via a modified Kurtz-Perry system at room temperature. The laser source was  $\text{Nd}^{3+}$ : YAG Q-switched solid-state laser with a wavelength of 1064 nm. The polycrystalline samples are divided 5 particle sizes through a screen mesh with different diameters: 38-55  $\mu\text{m}$ , 55-88  $\mu\text{m}$ , 88-105  $\mu\text{m}$ , 105-150  $\mu\text{m}$ , and 150-200  $\mu\text{m}$ , and then placed in an opaque box for laser irradiation. The intensity of SHG response light was collected by a photomultiplier tube, and KDP polycrystalline samples with the corresponding particle sizes were used as reference.

## 8. Theoretical calculations

First-principles calculations were performed to further analyse the structure-property relationship of  $\text{Pb}_2\text{B}_{10}\text{O}_{16}(\text{OH})_2 \cdot \text{B}(\text{OH})_3 \cdot \text{H}_2\text{O}$  via the plane-wave pseudopotential method implemented in the CASTEP software package.<sup>3</sup> The Perdew-Burke-Ernzerhof (PBE) functional under the generalized Gradient Approximation (GGA) was used to calculate the exchange-correlation potential.<sup>4</sup> The atom cutting radius are H: 0.32 Å, B: 0.88Å, O: 1.12Å, Pb: 1.47Å, Ba: 1.35Å, Ca: 0.99Å. The kinetic cutoff value in the normally conserved pseudopotential (NCP) is set at 820 eV to achieve energy convergence.<sup>5, 6</sup> The Monkhorst–Pack  $k$ -point meshes were set as  $3 \times 3 \times 4$  for  $\text{Pb}_2\text{B}_{10}\text{O}_{16}(\text{OH})_2 \cdot \text{B}(\text{OH})_3 \cdot \text{H}_2\text{O}$  in the Brillouin zone. Linear refractive index and birefringence can be obtained by the real part of the dielectric function according to band structure. In addition, the NLO coefficients were calculated at zero frequency using a formalism developed by Aversa and Sipe. The static second-order nonlinear coefficient  $\chi_{\alpha\beta\gamma}^{(2)}$  can be expressed as:

$$\chi_{\alpha\beta\gamma}^{(2)} = \chi_{\alpha\beta\gamma}^{(2)}(\text{VE}) + \chi_{\alpha\beta\gamma}^{(2)}(\text{VH}) \quad (1),$$

$$\chi_{\alpha\beta\gamma}^{(2)}(\text{VE}) = \frac{e^3}{2\hbar m^3} \sum_{vcc'} \int \frac{d^3k}{4\pi^3} P(\alpha\beta\gamma) \text{Im} [P_{cv}^\alpha P_{c'c'}^\beta P_{c'v'}^\gamma] \left( \frac{1}{\omega_{cv}^3 \omega_{v'c'}^2} + \frac{2}{\omega_{vc}^4 \omega_{c'v'}^4} \right) \quad (2),$$

$$\chi_{\alpha\beta\gamma}^{(2)}(\text{VH}) = \frac{e^3}{2\hbar m^3} \sum_{v'vc} \int \frac{d^3k}{4\pi^3} P(\alpha\beta\gamma) \text{Im} [P_{v'v}^\alpha P_{c'v'}^\beta P_{cv}^\gamma] \left( \frac{1}{\omega_{c'v'}^3 \omega_{vc}^2} + \frac{2}{\omega_{vc}^4 \omega_{c'v'}^4} \right) \quad (3).$$

Here,  $\alpha$ ,  $\beta$ , and  $\gamma$  are Cartesian components;  $v$  and  $v'$  represent valence bands;  $c$  and  $c'$  represent conduction bands, and  $P(\alpha\beta\gamma)$  is the full permutation. In addition,  $\hbar\omega_{ij}$  and  $P_{ij}^\alpha$  represent the band energy difference and the momentum matrix elements, respectively.



**Table S1.** Crystal data and structure refinement for  $\text{Pb}_2\text{B}_{10}\text{O}_{16}(\text{OH})_2\cdot\text{B}(\text{OH})_3\cdot\text{H}_2\text{O}$ .

Empirical formula	$\text{Pb}_2\text{B}_{10}\text{O}_{16}(\text{OH})_2\cdot\text{B}(\text{OH})_3\cdot\text{H}_2\text{O}$
Formula weight	892.35
Temperature	301(2) K
Wavelength	0.71073 Å
Crystal system, space group	Monoclinic, $P2_1$
Unit cell dimensions	$a = 6.6484(2)$ Å $b = 20.8682(7)$ Å $c = 6.7336(2)$ Å $\beta = 119.0742(11)$ °
Volume	816.50(4) Å <sup>3</sup>
Z, Calculated density	2, 3.630 g·cm <sup>-3</sup>
Absorption coefficient	20.721 mm <sup>-1</sup>
$F(000)$	804
Crystal size	0.11 × 0.04 × 0.03 mm <sup>3</sup>
Theta range for data collection	1.952 to 27.487 °
Limiting indices	$-7 \leq h \leq 8$ , $-26 \leq k \leq 27$ , $-8 \leq l \leq 8$
Reflections collected / unique	7404 / 3407 [ $R(\text{int}) = 0.0366$ ]
Completeness	99.80 %
Data / restraints / parameters	3407 / 19 / 318
Goodness-of-fit on $F^2$	0.968
Final $R$ indices [ $I > 2\sigma(I)$ ] <sup>[a]</sup>	$R_1 = 0.0273$ , $wR_2 = 0.0478$
$R$ indices (all data) <sup>[a]</sup>	$R_1 = 0.0320$ , $wR_2 = 0.0498$
Absolute structure parameter	0.015(15)
Extinction coefficient	0.00030(12)
Largest diff. peak and hole	1.336 and -1.189 e·Å <sup>-3</sup>

<sup>[a]</sup>  $R_1 = \sum||F_o| - |F_c|| / \sum|F_o|$  and  $wR_2 = [\sum w(F_o^2 - F_c^2)^2 / \sum wF_o^4]^{1/2}$  for  $F_o^2 > 2\sigma(F_o^2)$ .

**Table S2.** Atomic coordinates ( $\times 10^4$ ), equivalent isotropic displacement parameters ( $\text{\AA}^2 \times 10^3$ ), and BVS of each nonhydrogen atom for  $\text{Pb}_2\text{B}_{10}\text{O}_{16}(\text{OH})_2 \cdot \text{B}(\text{OH})_3 \cdot \text{H}_2\text{O}$ .  $U_{\text{eq}}$  is defined as one-third of the trace of the orthogonalized  $U_{ij}$  tensor.

Atoms	x	y	z	$U_{\text{eq}}$	BVS
Pb(1)	1752(1)	5593(1)	3723(1)	19(1)	1.50
Pb(2)	4903(1)	1781(1)	-770(1)	18(1)	1.48
B(1)	1770(30)	4061(9)	4150(30)	27(4)	3.18
B(2)	678(19)	5527(7)	-2175(19)	11(3)	3.05
B(3)	4960(20)	5295(10)	500(20)	17(3)	3.06
B(4)	5830(30)	4274(8)	2410(20)	18(3)	3.08
B(5)	6780(20)	5269(7)	4670(20)	14(3)	3.09
B(6)	7510(20)	5460(7)	8640(20)	15(3)	3.06
B(7)	8080(20)	2137(9)	6050(20)	15(3)	3.00
B(8)	3840(20)	1920(7)	3400(20)	17(3)	3.06
B(9)	690(20)	1986(7)	4250(20)	10(3)	3.01
B(10)	-60(20)	2155(7)	290(20)	11(3)	3.04
B(11)	-1030(30)	3151(8)	-1880(20)	19(3)	3.12
O(1)	1855(19)	3421(5)	4294(16)	38(3)	1.08
O(2)	870(20)	4415(6)	2210(17)	39(3)	1.31
O(3)	2499(19)	4455(5)	5961(15)	36(3)	1.24
O(4)	5799(18)	3624(5)	2275(15)	32(2)	1.03
O(5)	6871(14)	4575(4)	4459(14)	18(2)	1.79
O(6)	4772(15)	4604(5)	431(14)	18(2)	1.87
O(7)	-859(13)	5526(5)	-4430(12)	16(2)	2.05
O(8)	2962(13)	5587(6)	-1494(12)	16(2)	1.77
O(9)	-118(12)	5475(5)	-639(12)	16(2)	2.19
O(10)	7051(14)	5504(5)	374(13)	17(2)	1.76
O(11)	5173(12)	5560(5)	2585(11)	14(2)	1.86
O(12)	6035(13)	5414(4)	6407(12)	15(2)	2.08
O(13)	165(13)	1949(4)	5966(12)	17(2)	1.80

O(14)	3035(13)	1984(4)	4954(12)	16(2)	2.19
O(15)	-843(13)	2021(4)	1998(13)	16(2)	2.03
O(16)	2259(13)	1882(5)	1151(12)	17(2)	2.02
O(17)	6081(13)	1881(5)	4049(12)	15(2)	1.88
O(18)	70(17)	2857(5)	126(15)	22(2)	1.87
O(19)	-1678(12)	1859(5)	-1824(11)	8(2)	1.79
O(20)	-2079(17)	2857(5)	-3909(16)	18(2)	1.77
O(21)	-990(20)	3824(5)	-1758(16)	35(3)	0.92
O(22)	4668(19)	2922(5)	-1391(16)	40(3)	0.44

---



**Table S3.** Hydrogen coordinates ( $\times 10^4$ ) and isotropic displacement parameters ( $\text{Å}^2 \times 10^3$ ) for  $\text{Pb}_2\text{B}_{10}\text{O}_{16}(\text{OH})_2 \cdot \text{B}(\text{OH})_3 \cdot \text{H}_2\text{O}$

Atom	x	y	z	U(eq)
H(1)	1861	3087	3348	57
H(2)	182	4214	764	59
H(3)	3176	4497	7581	54
H(4)	5887	3308	3318	49
H(21)	-1565	4077	-3089	52
H(22A)	4655	3099	-261	60
H(22B)	3619	3098	-2559	60

**Table S4.** Hydrogen bonds for  $\text{Pb}_2\text{B}_{10}\text{O}_{16}(\text{OH})_2 \cdot \text{B}(\text{OH})_3 \cdot \text{H}_2\text{O}$ 

<b>D-H...A</b>	<b>d(H-A)/Å</b>	<b>d(D-A)/Å</b>	<b>D-H...A/°</b>
O(1)-H(1)...O(18)	1.96	2.727(13)	136.6
O(2)-H(2)...O(21)	1.69	2.641(14)	177.3
O(3)-H(3)...O(6)#3	1.7	2.649(12)	170.6
O(4)-H(4)...O(20)#4	1.94	2.761(14)	145
O(21)-H(21)...O(5)#5	1.79	2.729(13)	169.2
O(22)-H(22A)...O(4)	1.85	2.646(14)	154.7
O(22)-H(22B)...O(1)#1	1.98	2.783(14)	160.5

Symmetry transformations used to generate equivalent atoms:

#1  $x, y, z-1$     #2  $x+1, y, z$     #3  $x, y, z+1$     #4  $x+1, y, z+1$

#5  $x-1, y, z-1$     #6  $x-1, y, z$

**Table S5.** Bond lengths (Å) and angles (°) for Pb<sub>2</sub>B<sub>10</sub>O<sub>16</sub>(OH)<sub>2</sub>·B(OH)<sub>3</sub>·H<sub>2</sub>O.

Pb(1)-O(11)	2.731(7)	B(5)-O(11)	1.424(15)
Pb(1)-O(12)	2.552(8)	B(5)-O(12)	1.505(14)
Pb(1)-O(2)	2.617(12)	B(5)-O(5)	1.461(17)
Pb(1)-O(3)	2.725(11)	B(5)-O(7)#4	1.480(15)
Pb(1)-O(7)#3	2.584(7)	B(6)-O(10)#1	1.349(14)
Pb(1)-O(9)	2.585(7)	B(6)-O(9)#4	1.404(14)
Pb(2)-O(14)#1	2.556(7)	B(7)-O(13)#6	1.468(15)
Pb(2)-O(15)#2	2.569(8)	B(7)-O(17)	1.459(17)
Pb(2)-O(16)	2.649(7)	B(7)-O(19)#5	1.478(16)
Pb(2)-O(19)#2	2.695(7)	B(7)-O(20)#5	1.51(2)
Pb(2)-O(22)	2.409(11)	B(8)-O(14)	1.394(14)
B(1)-O(1)	1.34(2)	B(8)-O(16)	1.364(14)
B(1)-O(3)	1.35(2)	B(8)-O(17)	1.335(16)
B(2)-O(7)	1.357(13)	B(9)-O(13)	1.359(13)
B(2)-O(8)	1.362(13)	B(9)-O(14)	1.393(14)
B(2)-O(9)	1.376(13)	B(9)-O(15)	1.359(14)
B(3)-O(10)	1.501(16)	B(10)-O(15)	1.502(14)
B(3)-O(11)	1.449(14)	B(10)-O(16)	1.475(15)
B(3)-O(6)	1.45(2)	B(10)-O(18)	1.475(17)
B(3)-O(8)	1.484(16)	B(10)-O(19)	1.438(14)
B(4)-O(4)	1.36(2)	B(11)-O(18)	1.331(18)
B(4)-O(5)	1.360(16)	B(11)-O(20)	1.344(17)
B(4)-O(6)	1.353(17)	B(11)-O(21)	1.41(2)
O(22)-Pb(2)-O(14)#1	71.7(3)	O(15)-B(9)-O(14)	119.1(10)
O(22)-Pb(2)-O(15)#2	83.6(3)	O(13)-B(9)-O(14)	114.7(10)
O(14)#1-Pb(2)-O(15)#2	123.1(2)	O(19)-B(10)-O(16)	111.1(10)
O(22)-Pb(2)-O(16)	90.2(4)	O(19)-B(10)-O(18)	113.4(10)
O(14)#1-Pb(2)-O(16)	117.5(2)	O(16)-B(10)-O(18)	108.9(10)
O(15)#2-Pb(2)-O(16)	112.8(2)	O(19)-B(10)-O(15)	108.0(9)
O(22)-Pb(2)-O(19)#2	83.5(3)	O(16)-B(10)-O(15)	108.1(9)
O(14)#1-Pb(2)-O(19)#2	72.8(2)	O(18)-B(10)-O(15)	107.2(10)
O(15)#2-Pb(2)-O(19)#2	53.7(2)	O(7)-B(2)-O(8)	119.2(9)
O(16)-Pb(2)-O(19)#2	165.6(3)	O(7)-B(2)-O(9)	119.0(9)
O(12)-Pb(1)-O(7)#3	115.5(2)	O(8)-B(2)-O(9)	121.8(9)
O(12)-Pb(1)-O(9)	123.1(2)	O(18)-B(11)-O(20)	125.4(15)
O(7)#3-Pb(1)-O(9)	118.5(2)	O(18)-B(11)-O(21)	114.6(12)
O(12)-Pb(1)-O(2)	95.7(3)	O(20)-B(11)-O(21)	119.9(13)
O(7)#3-Pb(1)-O(2)	93.5(3)	O(11)-B(5)-O(5)	111.9(10)
O(9)-Pb(1)-O(2)	64.9(3)	O(11)-B(5)-O(7)#4	112.8(11)
O(12)-Pb(1)-O(3)	68.9(3)	O(5)-B(5)-O(7)#4	108.3(10)
O(7)#3-Pb(1)-O(3)	70.8(3)	O(11)-B(5)-O(12)	107.9(10)
O(9)-Pb(1)-O(3)	113.8(3)	O(5)-B(5)-O(12)	108.7(10)

O(2)-Pb(1)-O(3)	48.9(3)	O(7)#4-B(5)-O(12)	107.1(9)
O(12)-Pb(1)-O(11)	53.1(2)	O(6)-B(4)-O(4)	117.3(12)
O(7)#3-Pb(1)-O(11)	168.4(2)	O(6)-B(4)-O(5)	121.9(14)
O(9)-Pb(1)-O(11)	71.6(2)	O(4)-B(4)-O(5)	120.7(12)
O(2)-Pb(1)-O(11)	85.8(3)	O(1)-B(1)-O(3)	124.0(14)
O(3)-Pb(1)-O(11)	100.4(3)	O(1)-B(1)-O(2)	126.4(15)
O(6)-B(3)-O(11)	112.3(12)	O(3)-B(1)-O(2)	109.5(15)
O(6)-B(3)-O(8)	110.9(11)	O(12)-B(6)-O(10)#3	128.6(11)
O(11)-B(3)-O(8)	110.2(11)	O(12)-B(6)-O(9)#4	118.6(11)
O(6)-B(3)-O(10)	110.8(11)	O(10)#3-B(6)-O(9)#4	112.8(10)
O(11)-B(3)-O(10)	106.6(11)	O(17)-B(7)-O(13)#2	108.7(11)
O(8)-B(3)-O(10)	105.9(11)	O(17)-B(7)-O(19)#4	111.9(11)
O(17)-B(8)-O(16)	119.7(10)	O(13)#2-B(7)-O(19)#4	105.8(10)
O(17)-B(8)-O(14)	122.4(11)	O(17)-B(7)-O(20)#4	109.9(11)
O(16)-B(8)-O(14)	117.9(11)	O(13)#2-B(7)-O(20)#4	110.1(11)
O(15)-B(9)-O(13)	126.2(10)	O(19)#4-B(7)-O(20)#4	110.4(11)

---

Symmetry transformations used to generate equivalent atoms:

#1 x,y,z-1    #2 x+1,y,z    #3 x,y,z+1

#4 x+1,y,z+1    #5 x-1,y,z-1    #6 x-1,y,z

**Table S6.** Assignments of the infrared absorption bands for  $\text{Pb}_2\text{B}_{10}\text{O}_{16}(\text{OH})_2\cdot\text{B}(\text{OH})_3\cdot\text{H}_2\text{O}$

Assignments	Absorption bands ( $\text{cm}^{-1}$ )
asymmetric stretching of H-O in the [OH]	3379, 3259
the bending of group H-O-H in the $\text{H}_2\text{O}$	1639
asymmetric stretching of B-O in the $[\text{BO}_3]$	1369, 1242
asymmetric stretching vibrations of $[\text{BO}_4]$	1176, 1126, 1076, 983
symmetric stretching of B-O in the $[\text{BO}_3]$	929, 810
symmetric stretching of B-O in the $[\text{BO}_4]$	760
bending vibrations of $[\text{BO}_3]$	690, 621
bending vibrations of $[\text{BO}_4]$	597, 559

**Table S7.** A comprehensive study on the reported hydrated borates crystallized in noncentrosymmetric space groups containing Pb element

Compounds	Space groups	Band gaps (cutoff edges)	SHG effect (@1064 nm)	Phase matched	birefringence (@1064 nm)
$\text{Pb}_6\text{B}_{11}\text{O}_{18}(\text{OH})_9$ <sup>7</sup>	<i>P3</i> <sub>2</sub>	—	1.2×KDP	—	—
$\text{Pb}_6\text{B}_{12}\text{O}_{21}(\text{OH})_6$ <sup>8</sup>	<i>P3</i> <sub>2</sub>	—	—	—	—
$\text{Pb}_2\text{B}_3\text{O}_{5.5}(\text{OH})_2$ <sup>9</sup>	<i>Pnn2</i>	4.42 eV (280 nm)	3.0×KDP	Yes	—
$\text{Pb}_2[\text{B}_4\text{O}_5(\text{OH})_4](\text{OH})_2\cdot\text{H}_2\text{O}$ <sup>10</sup>	<i>C2</i>	—	60× $\alpha$ -SiO <sub>2</sub>	—	—
$\text{Pb}_2[\text{B}_5\text{O}_9]\text{Cl}\cdot 0.5\text{H}_2\text{O}$ <sup>11</sup>	<i>Pnn2</i>	—	—	—	—
$\text{Bi}_3[\text{B}_6\text{O}_{13}(\text{OH})]^{12}$	<i>P1</i>	—	1.5×KDP	—	—
$\text{Ba}_{2.16}\text{Pb}_{0.84}(\text{OH})(\text{B}_9\text{O}_{16})[\text{B}(\text{OH})_3]^{13}$	<i>P31c</i>	4.65 eV (267 nm)	1.2×KDP	Yes	—
$\text{Pb}_3(\text{OH})(\text{B}_9\text{O}_{16})[\text{B}(\text{OH})_3]^{13}$	<i>P31c</i>	4.58 eV (271 nm)	2.7×KDP	Yes	—
$\text{Pb}_2\text{B}_{10}\text{O}_{16}(\text{OH})_2\cdot\text{B}(\text{OH})_3\cdot\text{H}_2\text{O}$ (this work)	<i>P2</i> <sub>1</sub>	6.08 eV (204 nm)	2.1×KDP	Yes	0.067

—Not reported

**Table S8.** Dipole moment calculations of BO groups

Species	Compound	Dipole Moment(Debye)		
		x	y	z
BO groups	$\text{Pb}_2\text{B}_{10}\text{O}_{16}(\text{OH})_2 \cdot \text{B}(\text{OH})_3 \cdot \text{H}_2\text{O}$	0	11.39	0
	$\text{Ba}_2\text{B}_{10}\text{O}_{16}(\text{OH})_2 \cdot \text{B}(\text{OH})_3 \cdot \text{H}_2\text{O}$	0	5.86	0
	$\text{Ca}_2\text{B}_{10}\text{O}_{16}(\text{OH})_2 \cdot \text{B}(\text{OH})_3 \cdot \text{H}_2\text{O}$	0	-7.80	0

**Table S9.** Atom-cutting analysis of nonlinear coefficients  $d_{22}$ 

<b>Compound</b>	<b>total</b>	<b>Cut cation</b>	<b>Contribution percentage</b>
$\text{Pb}_2\text{B}_{10}\text{O}_{16}(\text{OH})_2 \cdot \text{B}(\text{OH})_3 \cdot \text{H}_2\text{O}$	0.42	0.16	62%
$\text{Ba}_2\text{B}_{10}\text{O}_{16}(\text{OH})_2 \cdot \text{B}(\text{OH})_3 \cdot \text{H}_2\text{O}$	-0.14	-0.11	21%
$\text{Ca}_2\text{B}_{10}\text{O}_{16}(\text{OH})_2 \cdot \text{B}(\text{OH})_3 \cdot \text{H}_2\text{O}$	0.12	0.05	58%



**Figure S1.** Powder XRD of  $\text{Pb}_2\text{B}_{10}\text{O}_{16}(\text{OH})_2 \cdot \text{B}(\text{OH})_3 \cdot \text{H}_2\text{O}$

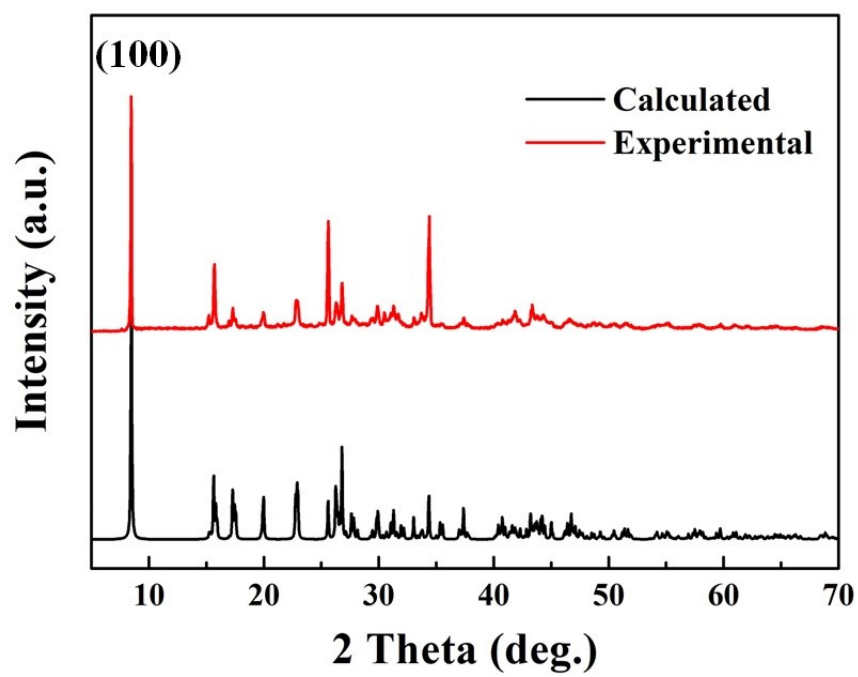


**Figure S2.** The arrangements diagrammatic drawing of lone pair electrons and link mode of Pb1 and Pb2 in  $\text{Pb}_2\text{B}_{10}\text{O}_{16}(\text{OH})_2\cdot\text{B}(\text{OH})_3\cdot\text{H}_2\text{O}$

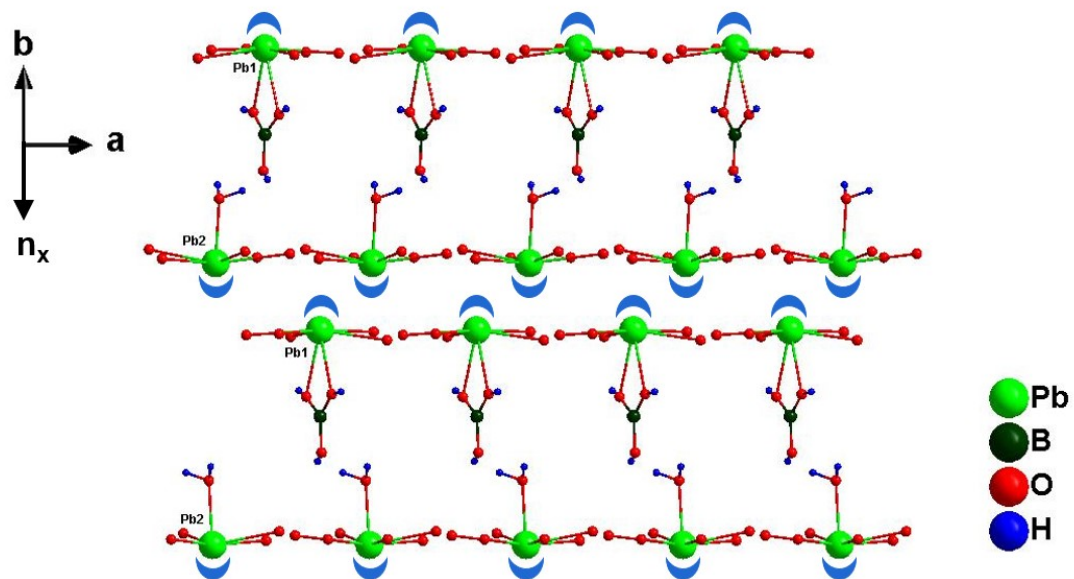


**Figure S3.** The distances between  ${}^2[B_5O_{10}(OH)]_\infty$  layers in (a)  $Pb_2B_{10}O_{16}(OH)_2 \cdot B(OH)_3 \cdot H_2O$ , (b)  $Ba_2B_{10}O_{16}(OH)_2 \cdot B(OH)_3 \cdot H_2O$ , (c)  $Sr_2B_{10}O_{16}(OH)_2 \cdot B(OH)_3 \cdot H_2O$  and (d)  $Ca_2B_{10}O_{16}(OH)_2 \cdot B(OH)_3 \cdot H_2O$

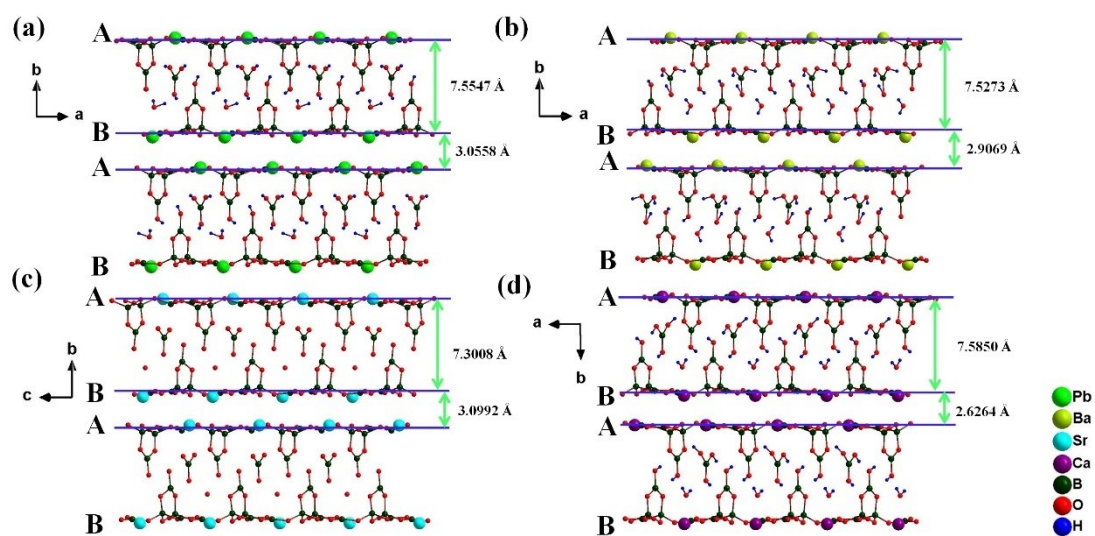


**Figure S4.** The shortest phase-matching length and calculated birefringence of  $\text{Pb}_2\text{B}_{10}\text{O}_{16}(\text{OH})_2 \cdot \text{B}(\text{OH})_3 \cdot \text{H}_2\text{O}$

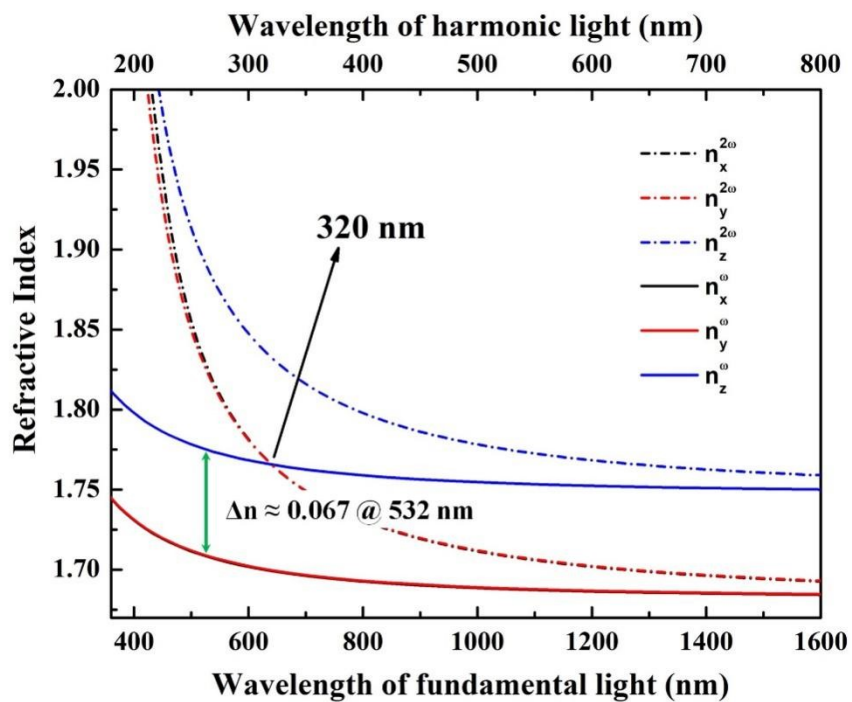
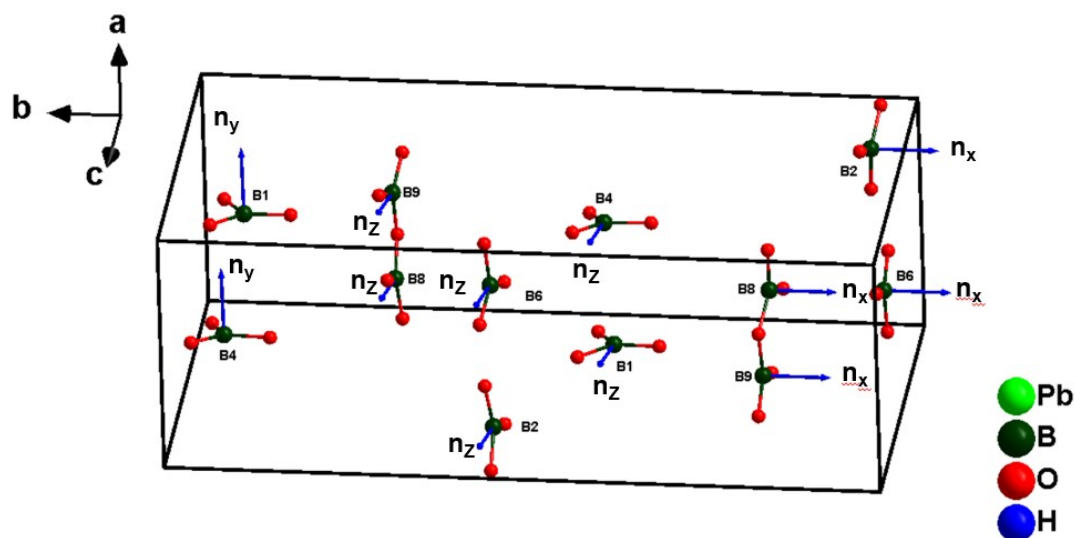


**Figure S5.** The arrangements of  $[\text{BO}_3]$  triangles and the  $n_x$ ,  $n_y$ ,  $n_z$  direction in  $\text{Pb}_2\text{B}_{10}\text{O}_{16}(\text{OH})_2\cdot\text{B}(\text{OH})_3\cdot\text{H}_2\text{O}$  unit cell



## Reference

1. G. Sheldrick, *Acta Crystallogr. A*, 2015, **71**, 3-8.
2. A. L. Spek, *J. Appl. Crystallogr.*, 2003, **36**, 7-13.
3. S. J. Clark, M. D. Segall, C. J. Pickard, P. J. Hasnip, M. I. Probert, K. Refson and M. C. Payne, *Z. Kristallogr.-Cryst. Mater.*, 2005, **220**, 567–570.
4. J. P. Perdew, K. Burke and M. Ernzerhof, *Phys. Rev. Lett.*, 1996, **77**, 3865.
5. J. S. Lin, A. Qteish, M. C. Payne and V. Heine, *Phys. Rev. B*, 1993, **47**, 4174.
6. A. M. Rappe, K. M. Rabe, E. Kaxiras and J. D. Joannopoulos, *Phys. Rev. B*, 1990, **41**, 1227.
7. Z.-T. Yu, Z. Shi, Y.-S. Jiang, H.-M. Yuan and J.-S. Chen, *Chem. Mater.*, 2002, **14**, 1314-1318.
8. S. Schöneegger, T. S. Ortner, K. Wurst, G. Heymann and H. Huppertz, *Z. Naturforsch. B*, 2016, **71**, 925-933.
9. J.-L. Song, C.-L. Hu, X. Xu, F. Kong and J.-G. Mao, *Inorg. Chem.*, 2013, **52**, 8979-8986.
10. A. G. Al-Ama, E. L. Belokoneva and S. Y. Stefanovich, *Russ. J. Inorg. Chem+*, 2005, **50**, 509-515.
11. J. Brugger, N. Meisser, S. Ansermet, S. V. Krivovichev, V. Kahlenberg, D. Belton and C. G. Ryan, *Am. Mineral.*, 2012, **97**, 1206–1212.
12. L. Y. Li, G. B. Li, Y. X. Wang, F. H. Liao and J. H. Lin, *Chem. Mater.*, 2005, **17**, 4174-4180.
13. J. J. Lu, G. Q. Shi, H. P. Wu, M. Wen, D. W. Hou, Z. H. Yang, F. F. Zhang and S. L. Pan, *RSC Adv.*, 2017, **7**, 20259-20265.